

EUROPEAN ORGANIZATION FOR NUCLEAR RESEARCH
Proposal to the ISOLDE and Neutron Time-of-Flight Committee

Study of ^{13}Be through isobaric analog resonances
in the Maya active target

January 5, 2011

R. Raabe¹, T. Roger¹, M. J. G. Borge², M. Caamaño³, D. Cortina-Gil³,
F. de Oliveira Santos⁴, B. Fernandez-Dominguez³, M. Freer⁵, H. O. U. Fynbo⁶,
L. Gaudefroy⁷, J. Gibelin⁸, G. F. Gryner⁴, A. Heinz⁹, J. S. Johansen⁶, B. Jonson⁹,
M. Marques⁸, W. Mittig¹⁰, E. Nacher², T. Nilsson⁹, G. Nyman⁹, N. Orr⁸, E. Pollacco¹¹,
K. Riisager⁶, P. Roussel-Chomaz¹², S. Sambri¹, H. Savajols⁴, O. Tengblad²,
M. Vandebrouck¹³, H. Wang¹⁰

¹*Instituut voor Kern- en Stralingsfysica, K.U.Leuven, Celestijnenlaan 200d - B-3001 Leuven*

²*Instituto de Estructura de la Materia, CSIC, Serrano 113bis, E-28006-Madrid, Spain*

³*Universidade de Santiago de Compostela, E-15782 Santiago de Compostela, Spain*

⁴*Grand Accélérateur National d'Ions Lourds, B.P. 55027, F-14076 Caen Cedex 05, France*

⁵*School of Physics and Astronomy, University of Birmingham, Birmingham B15 2TT, United Kingdom*

⁶*Department of Physics and Astronomy, University of Aarhus, Ny Munkegade 1520, DK-8000 Aarhus C, Denmark*

⁷*CEA/DAM/DIF, F-91297 Arpajon, France*

⁸*LPC-ENSICAEN, IN2P3/CNRS et Université de Caen, 14050 Caen, France*

⁹*Fundamental Physics, Chalmers University of Technology, S-412 96 Göteborg, Sweden*

¹⁰*Department of Physics and Astronomy, National Superconducting Cyclotron Laboratory, Michigan State University, East Lansing, Michigan 48824, USA*

¹¹*CEA/IRFU/SPhN, 91191 Gif-sur-Yvette, France*

¹²*CEA/DSM/Direction, 91191 Gif-sur-Yvette, France*

¹³*Institut de Physique Nucléaire, Université Paris-Sud, IN2P3-Centre National de la Recherche Scientifique, F-91406 Orsay CEDEX, France*

Spokesperson: Riccardo Raabe [raabe@kuleuven.be]
Contact person: Thierry Stora [thierry.stora@cern.ch]

Abstract: We propose to perform an experiment with a ^{12}Be beam and the Maya active target. We intend to study the ground state of ^{13}Be through the population of its isobaric analog resonance in ^{13}B . The resonance will be identified detecting its proton- and neutron-decay channels.

Requested shifts: 40 shifts, (split into 1 runs over 1 year) + 1 day test



1 Introduction

The neutron-rich Be beams available at ISOLDE offer a unique opportunity to study the properties of these light nuclei. Our interest focuses here on the unbound system ^{13}Be . Determination of the sequence of its low-lying states can shed light on the evolution of the $N = 8$ shell closure towards the dripline, as well as provide important information for the modelling of the two-neutron halo nucleus ^{14}Be [1, 2].

In ^{13}Be , a resonance was observed for the first time, at about 2 MeV above the neutron-emission threshold, in the $^{14}\text{C}(^7\text{Li}, ^8\text{B})$ reaction [3]. The resonance was then confirmed in essentially all further measurements [4–11]. The double-charge exchange measurement $^{13}\text{C}(^{14}\text{C}, ^{14}\text{O})$ of Ref. [4] and the (d, p) transfer reaction of Ref. [5] consistently identified the 2-MeV resonance as a $d_{5/2}$ state. The situation regarding other, lower-lying states is more controversial. In the multi-nucleon transfer $^{14}\text{C}(^{11}\text{B}, ^{12}\text{N})^{13}\text{Be}$ [6] a narrow resonance at 800 keV above the neutron emission threshold was assigned the spin $J = 1/2$ but without resolving the parity. Later, a broad structure at a similar [7] or lower energy [8–10] was observed in projectile fragmentation measurements and interpreted as an s -state, with significant differences regarding its characteristics (virtual state or resonance due to a deformation of the ^{12}Be core). A very recent result from a one-neutron removal cross section [11] confirms a broad s virtual state at low energy, and places the $p_{1/2}$ resonance at 510 keV: this low-lying “intruder” state implies the strong reduction of the gap between the $1p_{1/2}$ orbital and the $2s_{1/2}$ orbital ($N = 8$ shell).

Several theoretical works concentrated on ^{13}Be and the ^{12}Be - n interaction, especially as building blocks for ^{14}Be . It was early realized that, if the normal ordering of shells and an unbound s -ground state of ^{13}Be is assumed, the $d_{5/2}$ resonance would have to be lower than the observed 2 MeV in order to reproduce the two-neutron separation energy in ^{14}Be [2]. The discrepancy can be solved by an inversion of the $2s_{1/2}$ and $1p_{1/2}$ shells, as occurring in ^{11}Be and ^{10}Li [12–14]. Other works [15–17] managed to reproduce the characteristics of ^{13}Be and ^{14}Be with a $1/2^+$ resonance very close to the neutron emission threshold and a $5/2^+$ resonance at the observed energy, by including excitations or deformations of the ^{12}Be core in the models.

It is clear that more experimental information is needed in order to solve the questions about the low-lying states in ^{13}Be .

2 Method

Resonant scattering on protons [18] is an established method to study excited and unbound states near the proton dripline (see for example [19]). The method is based on the dominance of resonance scattering over other reactions that could be sources of background. On the neutron-rich side, the needed information can be obtained through the study of isobaric analog states (IAS) [18, 20]. Once the IAS is populated, isospin conservation allows proton decay (to the entrance channel) and isospin-symmetric neutron decay, where the remaining nucleus is the IAS of the beam nucleus: see Fig. 1 for the case of ^{13}Be . The wave function of the states with $T = 5/2$ in ^{13}B can be written as [22]:

$$\Psi_{^{13}\text{B}(T=5/2)} = \frac{1}{\sqrt{5}} (\Psi_{^{12}\text{Be}+p} + 2 \times \Psi_{^{12}\text{B}+n}) ,$$

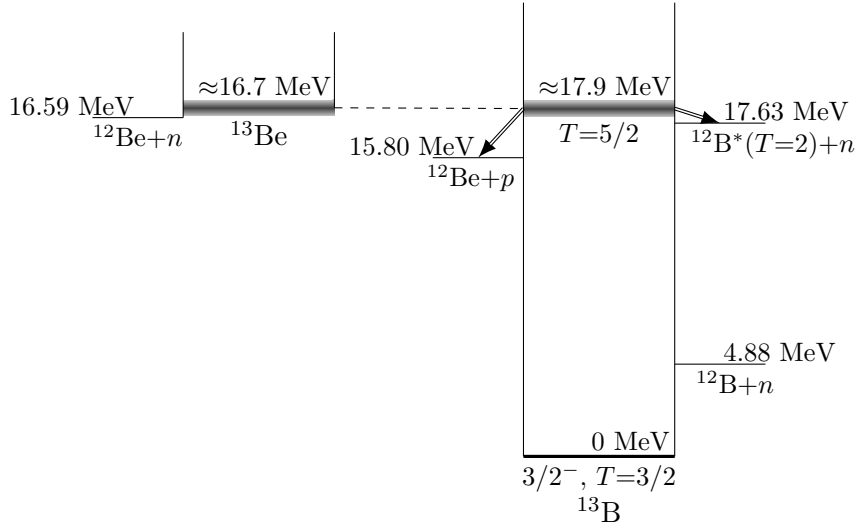


Figure 1: Isobar diagram for $A = 13$ Be and B nuclei. Energies are calculated from the 2003 Atomic Mass Evaluation [21]. The diagrams for individual isobars have been shifted vertically to eliminate the neutron-proton mass difference and the Coulomb energy, taken as $E_C = 0.60 \times Z(Z - 1)/A^{1/3}$. The IAS of ^{13}Be in ^{13}B is placed at ≈ 17.9 MeV based on the systematics in $A = 13$ nuclei. When the IAS is populated in resonant scattering on protons, isospin conservation allows it to decay to the entrance channel $^{12}\text{Be} + p$ and to its conjugate $^{12}\text{B}^*(T=2) + n$.

from which it follows that the neutron decay is four times more probable than the proton decay. The actual decay rates to the two channels will also be determined by phase space and penetrability factors.

It is clear that detection of both the neutron-emission and proton-emission channels are desirable. For the latter, charged-particle silicon detectors are usually employed at forward angles, ensuring a good efficiency. For the former channel, Rogachev et al. [23] have employed neutron detectors, to measure the $^6\text{He}(p,n)^6\text{Li}^*(0^+;T=1)$ reaction populating the ^7He IAS in ^7Li . Coincident detection of γ -rays from the decay of $^6\text{Li}^*$ ensured the identification of the channel of interest. In a successive measurement [24], the same group extracted the information about the emitted neutrons directly from the Doppler-shifted γ -rays. The experiments proved the potential of the method, as this decay channel becomes very important in neutron-rich nuclei. However, the efficiency for the detection of the emitted neutrons becomes an important issue if the technique is to be applied to more exotic nuclei, for which beams are available at very low intensities. The use of an active target offers a solution to this problem, and a way to detect both decay channels simultaneously.

The MAYA active target [25] is a gaseous detector, providing three-dimensional reconstruction of the tracks of the charged particles traversing the gas volume (see Fig. 2). The electrons created by ionisation drift in an electric field towards an amplification zone (wire plane) where they create avalanches; the mirror charges are collected on a honeycomb-segmented cathode creating a two-dimensional projection of the tracks. The

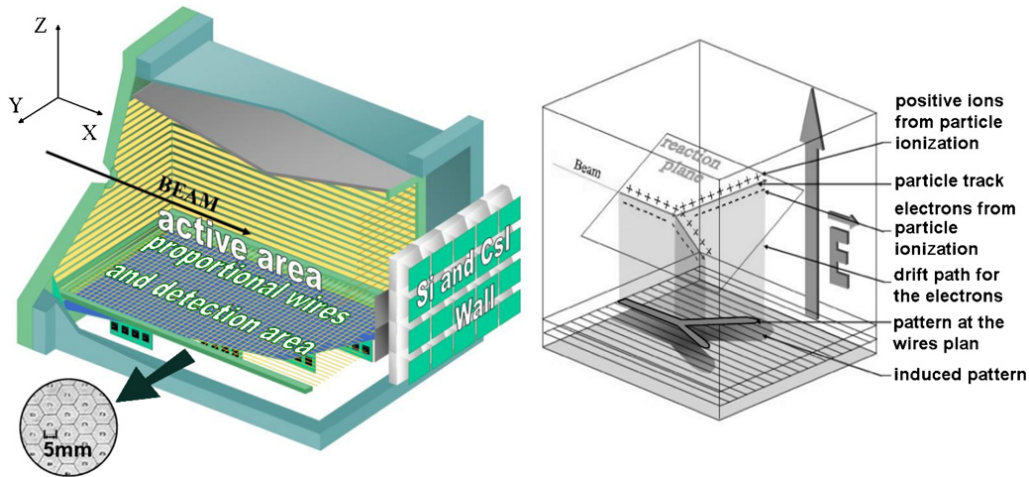


Figure 2: Schematic design of the MAYA detector and working principle.

third dimension is obtained from the drift time of the electrons. Identification of the particles is achieved via the specific energy loss, the total energy deposited and the length of the paths. An array of Si and CsI detectors covers the wall opposite to the beam entrance, to detect forward-emitted light ions which are not stopped in the gas volume. The detection gas is chosen so that the nuclei of its atoms act at the same time as targets for the reaction of interest. MAYA has been used in a number of configurations: with isobutane (C_4H_{10}) at various pressures for reactions on ^{12}C [26] or on protons [27, 28], with deuterium for (d,d') reactions [29]; very recently, a mixture of He (98%) and CF_4 (2%) has also been successfully used to study inelastic scattering on 4He .

For the problem at hand, both a (p,p) scattering and a (p,n) reaction can be identified in MAYA, by the direct detection of the recoil proton, and by looking at the change in the energy deposition of the beam-like particles, respectively. By properly tuning the gas pressure, the Z -charged beam particles, which do not undergo a reaction, traverse the volume losing their energy (thus scanning the resonant region above the proton-decay threshold) and are detected in the silicon wall opposite the entrance. On the other hand, both in the case of a resonant elastic scattering and a (p,n) reaction (where the $Z+1$ IAS of the beam particle is produced), the beam-like particles emerge with a lower energy and are subsequently stopped in the gas volume. The energies of the beam-like particles in case of an elastic scattering or a (p,n) reaction is similar, since the (negative) Q -value of the latter process is small with respect to the kinetic energy of the beam.

Protons recoiling from the elastic scattering events will be detected in the solid-state array placed at forward angles. Their energy and angle, together with the path length of the beam-like particle, provide the means for the kinematic reconstruction, and thus extraction of the centre-of mass scattering energy.

A (p,n) reaction, on the other hand, can be identified by looking at the specific energy loss, which is higher for the $Z+1$ particle produced in the process. The situation is illustrated in Fig. 3, which shows the results of a test measurement performed with a 6He beam at GANIL [30]. For example the maximum energy loss at the Bragg peak (Q_P in Fig. 3),

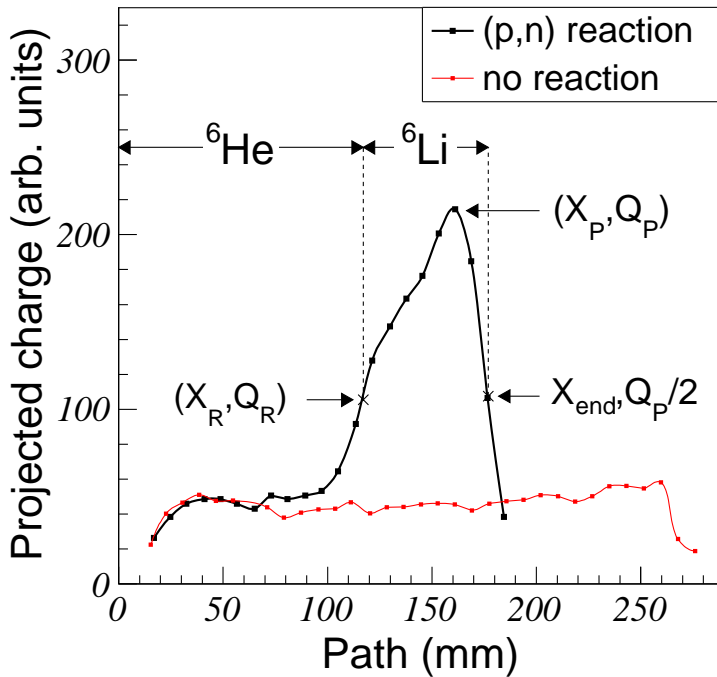


Figure 3: Example of a beam-direction projected charge profile for an event without a reaction (red curve) and a ${}^6\text{He}(p,n){}^6\text{Li}^*$ (IAS) reaction (black curve) [30]. The parameters, used for the identification of events, are indicated.

which depends on Z , is compared along the path of a non-reacting particle and a reacting one, obtaining a clear identification. From the identified events, the centre-of-mass energy at which the reaction occurred is calculated from the position of the interaction (X_R in Fig. 3).

The yield of the two kind of events as function of the centre-of-mass energy provides the excitation function. For example, the result for the ${}^6\text{He}(p,n){}^6\text{Li}^*(T=1)$ reaction is shown in Fig. 4. The resonance values extracted from the fit are in agreement, within one standard deviation, with those from Ref. [23], improving slightly on the uncertainties. It is important to stress that the excitation function was obtained using only 5×10^6 incident particles *in total*, thanks to a detection efficiency for the channel of interest of 80%.

3 Experimental Details

The MAYA detector will be placed at the end of an available beam line after the REX post-accelerator. It will be filled with isobutane (C_4H_{10}) at a pressure of about 100 mbar. With this choice, the incoming ${}^{12}\text{Be}$ ions ($E_{\text{beam}} = 3$ MeV/nucleon) will traverse the gas volume, probing the reaction energies between ≈ 2.9 MeV/nucleon and ≈ 0.7 MeV/nucleon. This translates in a scan of excitation energies in ${}^{13}\text{B}$ from 16.5 MeV to 18.5 MeV (see Fig. 1), thus covering the region of interest.

Protons from resonant elastic scattering will be detected with good efficiency for centre-of-mass angles larger than ≈ 90 degrees (corresponding to forward-emitted protons), thanks

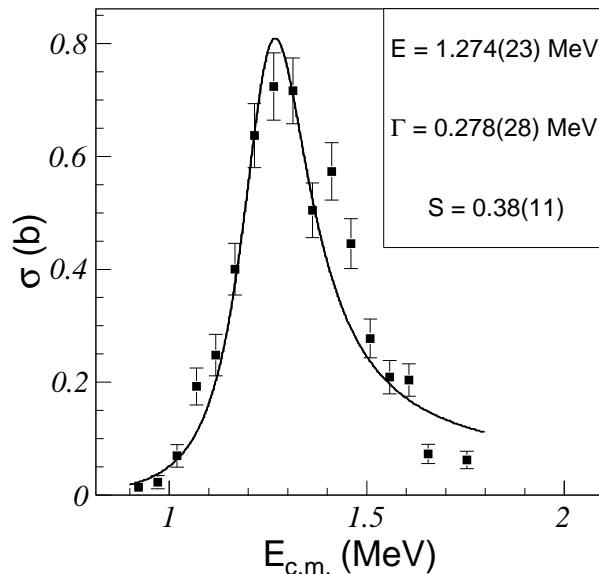


Figure 4: Excitation function for the ${}^6\text{He}(p,n){}^6\text{Li}^*(T=1)$ [30]. The curve is a fit made with a (modified) Breit-Wigner function, providing the resonance parameters $E_r = 1.274(23)$ MeV, $\Gamma = 0.278(28)$ MeV.

to the charged-particle Si+CsI telescopes placed on the wall opposite to the beam entrance.

The neutron decay of the IAS, ${}^{12}\text{Be}(p,n){}^{12}\text{B}^*(T=2)$, will be identified as described in the previous section, thanks to the different energy loss of ${}^{12}\text{Be}$ and ${}^{12}\text{B}$ nuclei in the gas. The expected detection efficiency is around $\epsilon = 80\%$ for the quoted energy range.

Reconstruction of the centre-of-mass energy is based on the determination of the reaction point: using interpolation algorithms on the deposited charge, a spatial resolution of 1 mm or better can be achieved [31], translating to less than 10 keV uncertainty in energy. A larger contribution to the uncertainty is expected from the spread in the incoming beam energy (30 keV for a spread of 300 keV).

We base our beam time estimate on the neutron-emission channel, which we expect to be the most important. We aim at building an excitation function over 2 MeV in steps of 50 keV, with an error better than 10% for a cross section $\sigma \approx 0.4$ b (see Fig. 4). A bin of 50 keV (in the centre of mass) corresponds to about 5 mm of gas at 100 mbar, or a thickness $N\Delta x \approx 5 \times 10^{18}$ protons/cm². For the beam intensity we take an estimate $I = 50$ pps (see also further). To reach a yield $Y = 100$ counts in a 50-keV bin we would then need

$$\Delta t = \frac{Y}{I \times N\Delta x \times \sigma \times \epsilon} = \frac{100}{50 \times 5 \times 10^{18} \times 0.4 \times 10^{-24} \times 0.8} \text{ s} \approx 12 \text{ days.}$$

The time structure of the beam at REX imposes strong constraints on the use of the MAYA active target. Depending on the settings of the EBIS source and the post-accelerator, the instantaneous rate can be up to three orders of magnitude higher than the average intensity: in this case, a few 10^4 pps. MAYA has already been used at these beam intensities (see for example Ref. [29]), and the limit, at which space-charge effects may

lead to a constant discharge in the gas volume, is one order of magnitude higher.

An important problem for the proposed measurement is represented by the contamination of $^{12}\text{C}^{4+}$ in the ^{12}Be beam. A recent measurement has shown currents of the order of a few particle-pA [32]. The use of a stripper foil at the end of REX, used in a test in 2005 [33], has brought a reduction of a factor ≈ 100 ; this, however, is still not sufficient for our purposes. A proposed method for a drastic reduction [34] consists in placing another stripper foil after the RFQ element in REX. This configuration could be tested with one day of ^9Be stable beam.

4 Summary and Beam Time Request

We intend to study the ^{13}Be nucleus through the population of its IAS in ^{13}B . The state will be investigated via the allowed neutron and proton decays, detected in the MAYA active target. The technique allows measuring the excitation function with good accuracy using a very weak ^{12}Be beam of only 50 pps.

We estimate about 12 days of data taking to achieve this goal. Based on our experience with MAYA, usually one-two days are spent tuning the parameters (gas pressure, electron amplification settings); this would be done with a more intense beam, but with the same Z as the one of interest. By using a radioactive beam, the same time could be used for the conditioning of the target. We therefore ask a total of 40 8-hour shifts.

This is summarised in the table below.

Beam	Min. Intensity	Target	Ion Source	Shifts
^{12}Be	20 pps	Ta	RILIS	36
^{10}Be	100 pps	Ta	RILIS	4

Preliminary to the actual experiment, we will need to perform a test, to check a possible method for the elimination of the $^{12}\text{C}^{4+}$ contaminant in the ^{12}Be beam. This would require **one day** of ^9Be stable beam.

- [1] G. F. Bertsch and H. Esbensen, *Ann. Phys. (New York)* **209**, 327 (1991).
- [2] I. J. Thompson and M. V. Zhukov, *Phys. Rev. C* **53**, 708 (1996).
- [3] D. V. Aleksandrov *et al.*, *Sov. J. Nucl. Phys.* **37**, 474 (1983).
- [4] A. N. Ostrowski *et al.*, *Z. Phys. A* **343**, 489 (1992).
- [5] A. A. Korshennikov *et al.*, *Phys. Lett. B* **343**, 53 (1995).
- [6] A. V. Belozorov *et al.*, *Nucl. Phys. A* **636**, 419 (1998).
- [7] J. L. Lecouey, *Few-Body Syst.* **34**, 21 (2004).
- [8] M. Thoennessen, S. Yokoyama, and P. G. Hansen, *Phys. Rev. C* **63**, 014308 (2000).
- [9] H. Simon *et al.*, *Nucl. Phys. A* **791**, 267 (2007).
- [10] G. Christian *et al.*, *Nucl. Phys. A* **801**, 101 (2008).

- [11] Y. Kondo *et al.*, Phys. Lett. B **690**, 245 (2010).
- [12] M. Labiche, F. M. Marques, O. Sorlin, and N. Vinh Mau, Phys. Rev. C **60**, 027303 (1999).
- [13] J. C. Pacheco and N. Vinh Mau, Phys. Rev. C **65**, 044004 (2002).
- [14] G. Blanchon *et al.*, Phys. Rev. C **82**, 034313 (2010).
- [15] P. Descouvemont, Phys. Lett. B **331**, 271 (1994).
- [16] A. Adahchour, D. Baye, and P. Descouvemont, Phys. Lett. B **356**, 445 (1995).
- [17] T. Tarutina, I. J. Thompson, and J. A. Tostevin, Nucl. Phys. A **733**, 53 (2004).
- [18] V. Z. Goldberg, in *Exotic nuclei and atomic masses (ENAM 98)* (AIP Conference Proceedings, 1998), Vol. 455, p. 319.
- [19] L. Axelsson *et al.*, Phys. Rev. C **54**, R1511 (1996).
- [20] G. V. Rogachev *et al.*, Phys. Rev. C **67**, 041603 (2003).
- [21] G. Audi, A. H. Wapstra, and C. Thibault, Nucl. Phys. A **729**, 337 (2003).
- [22] A. Bohr and B. R. Mottelson, *Nuclear Structure* (Benjamin, 1969).
- [23] G. V. Rogachev *et al.*, Phys. Rev. Lett. **92**, 232502 (2004).
- [24] P. Boutachkov *et al.*, Phys. Rev. Lett. **95**, 132502 (2005).
- [25] C. E. Demonchy *et al.*, Nucl. Instrum. Methods Phys. Res. A **573**, 145 (2007).
- [26] M. Caamaño *et al.*, Phys. Rev. C **78**, 044001 (2008).
- [27] I. Tanihata *et al.*, Phys. Rev. Lett. **100**, 192502 (2008).
- [28] T. Roger *et al.*, Phys. Rev. C **79**, 031603(R) (2009).
- [29] C. Monrozeau *et al.*, Phys. Rev. Lett. **100**, 042501 (2008).
- [30] T. Roger *et al.*, in preparation.
- [31] T. Roger, Ph.D. thesis, Université de Caen / Basse Normandie, 2009.
- [32] F. Wenander, J. Instrum. **5**, C10004 (2010).
- [33] K. Riisager, private communication.
- [34] F. Wenander, private communication.

Appendix

DESCRIPTION OF THE PROPOSED EXPERIMENT

The experimental setup comprises: (*name the fixed-ISOLDE installations, as well as flexible elements of the experiment*)

Part of the	Availability	Design and manufacturing
REX post-accelerator	<input checked="" type="checkbox"/> Existing	<input checked="" type="checkbox"/> To be used without any modification
Maya active-target detector	<input checked="" type="checkbox"/> Existing	<input checked="" type="checkbox"/> To be used without any modification <input type="checkbox"/> To be modified
	<input type="checkbox"/> New	<input type="checkbox"/> Standard equipment supplied by a manufacturer <input type="checkbox"/> CERN/collaboration responsible for the design and/or manufacturing
Maya gas supply system	<input checked="" type="checkbox"/> Existing	<input checked="" type="checkbox"/> To be used without any modification <input type="checkbox"/> To be modified
	<input type="checkbox"/> New	<input type="checkbox"/> Standard equipment supplied by a manufacturer <input type="checkbox"/> CERN/collaboration responsible for the design and/or manufacturing

HAZARDS GENERATED BY THE EXPERIMENT (if using fixed installation:) Hazards named in the document relevant for the fixed [COLLAPS, CRIS, ISOLTRAP, MINIBALL + only CD, MINIBALL + T-REX, NICOLE, SSP-GLM chamber, SSP-GHM chamber, or WITCH] installation.

Additional hazards:

Hazards	Maya active-target detector	Maya gas supply system	—
Thermodynamic and fluidic			
Pressure	Isobutane (C ₄ H ₁₀), ≈100 mbar, ≈20 l, static mode. Separation from the vacuum of the beam line with a mylar window. An automatic safety valve will be installed on the beam line to prevent accidental escape of the gas.	Access to isobutane (one cylinder).	
Vacuum			
Temperature	room temperature (monitored)	room temperature	
Heat transfer			
Thermal properties of materials			
Cryogenic fluid			

Electrical and electromagnetic			
Electricity			
Static electricity	Static electric field in the detector: typically 100 V/cm		
Magnetic field			
Batteries	<input type="checkbox"/>		
Capacitors	<input type="checkbox"/>		
Ionizing radiation			
Target material			
Beam particle type (e, p, ions, etc)	ions: ^{10}Be , $T_{1/2} = 1.5 \times 10^6$ y. ^{12}Be , $T_{1/2} = 21.5$ ms,		
Beam intensity	100 pps max		
Beam energy	3 MeV/nucleon		
Cooling liquids			
Gases			
Calibration sources:	<input checked="" type="checkbox"/>		
• Open source	<input type="checkbox"/>		
• Sealed source	<input checked="" type="checkbox"/> [ISO standard]		
• Isotope	Am-Cu-Pu		
• Activity	≈ 5 kBq		
Use of activated material:	No		
• Description	<input type="checkbox"/>		
• Dose rate on contact and in 10 cm distance			
• Isotope			
• Activity			
Non-ionizing radiation			
Laser			
UV light			
Microwaves (300MHz-30 GHz)			
Radiofrequency (1-300 MHz)			
Chemical			
Toxic			
Harmful			
CMR (carcinogens, mutagens and substances toxic to reproduction)			
Corrosive			

Irritant			
Flammable	isobutane		
Oxidizing			
Explosiveness			
Asphyxiant			
Dangerous for the environment			
Mechanical			
Physical impact or mechanical energy (moving parts)			
Mechanical properties (Sharp, rough, slippery)			
Vibration			
Vehicles and Means of Transport			
Noise			
Frequency			
Intensity			
Physical			
Confined spaces			
High workplaces			
Access to high workplaces			
Obstructions in passageways			
Manual handling			
Poor ergonomics			

Hazard identification:
 Flammable gas: isobutane

Average electrical power requirements (excluding fixed ISOLDE-installation mentioned above):
 ≈ 1 kW